Turkish J. Eng. Env. Sci.
29 (2005) , 129 – 142.
© TÜBİTAK

Investigation of Methanol Oxidation on Polycrystalline Pt: Importance of the Water-Gas Shift Reaction

Niyazi Alper TAPAN
Gazi University, Department of Chemical Engineering,
Ankara-TURKEY
e-mail: atapan@gazi.edu.tr
Jai PRAKASH
Department of Chemical and Environmental Engineering,
Illinois Institute of Technology, Chicago, Illinois, USA

Received 30.03.2004

Abstract

A water-gas shift reaction model was proposed for methanol oxidation on polycrystalline platinum. To see if the model proposed can explain methanol oxidation on platinum metal, a polycrystalline platinum electrode was used and simulations were compared with the chronoamperometric experiments at different applied potentials, E < 0.6 V. The pseudo steady state hypothesis model shows that at E < 0.6 V the water gas shift reaction can explain the methanol oxidation. After 0.45 V the rate-determining step shifted from a water-gas shift reaction to third decomposition and CO formation. Dynamic profiles showed that surface CO, CHO and CH_2O show completely different profiles from PSSH. The water-gas shift reaction was always the rate-determining step in the potential range studied with oxidation times of less than 1 s.

Key words: Water-gas shift, Methanol, Oxidation, Platinum, Carbon monoxide.

Introduction

Even after more than 30 years of fundamental studies, the mechanism of the oxidation of methanol is still not well understood; this is a factor hindering the development of the Direct Methanol Fuel Cell (Beden *et al.*, 2001; Lamy *et al.*, 2001).

For many years, research by numerous electrochemical and surface science groups focused on catalytic decomposition of methanol on platinum, which is a model surface for fundamental studies. Several mechanisms were proposed for the oxidation of methanol on a platinum surface. The first mechanism proposed for the oxidation of methanol was the Bagotzky scheme (Bagotzky *et al.*, 1977), where methanol was decomposed to carbon monoxide by 6 different steps starting from the C-H bond. Although it is thought that methanol starts to decompose from the methyl end of the molecule (Ehlers *et al.*, 1985; Franaszczuk *et al.*, 1992) OH bond breakage is still a possible initiation step for methanol decomposition (Beden *et al.*, 2001; Lipkowski and Ross, 2001). After Bagotzky, parallel and series mechanisms were proposed, where methanol decomposes to either carbon monoxide or carbon dioxide following different or the same pathways (Vieltich and Xia, 1995; Jarvi *et al.*, 1997; Wieckowski *et al.*, 2000).

After several mechanistic studies, researchers came to some conclusions about methanol oxidation, stating that methanol decomposition following its catalytic activation is irreversible. Before the electrochemical activation of water (0.6 V vs. RHE), above a critical potential (0.3 V vs. RHE) threshold, surface carbon monoxide starts to decompose to carbon dioxide. Before this critical potential, current transient for methanol oxidation decays to zero and after that current reaches a steady state (Wieckowski *et al.*, 2000).

In order to see how methanol decomposes before and after 0.3 V vs. RHE, we proposed a 4-step mechanism for the decomposition of methanol and a water-gas shift reaction for the oxidation of carbon monoxide.

$$Pt + CH_3OH \rightarrow Pt - (CH_3OH)_{ads} \quad (1)$$

$$Pt - (CH_3OH)_{ads} \rightarrow Pt - (CH_3O)_{ads} + H^+ + e - \quad (2)$$

$$Pt - (CH_3O)_{ads} \rightarrow Pt - (CH_2O)_{ads} + H^+ + e - \quad (3)$$

$$Pt - (CH_2O)_{ads} \rightarrow Pt - (CHO)_{ads} + H^+ + e - \quad (4)$$

$$Pt - (CHO)_{ads} \rightarrow Pt - (CO)_{ads} + H^+ + e - \quad (5)$$

$$Pt + H_2O \rightarrow Pt - -(H_2O) \quad (6)$$

$$Pt - (CO)_{ads} + M - -(H_2O) \rightarrow Pt + M + CO_2 + 2H^+ + 2e^- \quad (7)$$

In this model, all intermediate species are assumed to occupy only one site on the platinum surface. To see if the model proposed can explain methanol oxidation on platinum metal, we used a polycrystalline platinum electrode and compared our simulation with the chronoamperometric experiments at different applied potentials, E < 0.6 V.

In order to determine the electrokinetic rate constants for the assumed methanol electro-oxidation mechanism, we applied a pseudo steady state hypothesis (Fogler, 1999). In order to apply a steady state model on the platinum surface, we carried out chronoamperometric experiments to find the steady state currents for the specified range of cell potential. Steady state currents were used to estimate the rate constants in the proposed mechanism, which helped us to determine the dynamic profile of surface poisoning on the platinum surface.

Experimental

Determination of active sites on the polycrystalline platinum electrode

The experiments were carried out in a glass cell with a main compartment for the working electrode and 2 separate small compartments for the counter and reference electrodes plus a Luggin capillary for the latter to minimize IR drop. Successive stages of mechanical polishing of the electrode were carried out with 0.05 μm γ-alumina powder (Buehler Ltd.). A Buehler microcloth was used for polishing with alumina and ultrapure water was used as lubricant and wash. After a mirror finish was achieved, the electrode was cleaned ultrasonically in ultrapure water to remove alumina particles. For subsequent experiments, only polishing with water-paste of 0.05 μm γ-alumina was repeated and the surface was then cleaned ultrasonically (Prakash *et al.*, 2000). In order to avoid background currents originating from dissolved oxygen, the electrolyte was purged and blanketed with argon. Solutions of 0.5M H_2SO_4 + CH_3OH were prepared from high purity sulfuric acid and high purity grade methanol, and deionized water. The electrolyte was deaerated with ultra-high-purity argon (99.999%) before and during the experiments.

The working electrode was a polycrystalline platinum electrode with 2 mm in diameter that was polished with 0.1 and 0.05 μm Al_2O_3 paste and washed ultrasonically for 1 h in deionized water. A larger area Pt foil was used as a counter electrode. All potentials were measured against a standard calomel electrode (SCE).

A 3-compartment electrochemical cell (40 ml) equipped with a Luggin capillary and CHI660 potentiostat interfaced to a PC were used. Chronoamperometric data were collected at sampling rates of 50ms per point. The chemicals were Millipore water (18 MΩ cm) and high purity sulfuric acid, ACS (American Chemical Society) certified methanol (99.9% pure). The experiments were carried out at room temperature (25 °C).

A potentiodynamic sweep was applied to a Pt electrode in H_2SO_4 to obtain a current-potential curve from which the quantity of chemisorbed H_2 was determined (Kinoshita *et al.*, 1986). A potentiodynamic current-potential curve for a polycrystalline Pt is shown in Figure 1.

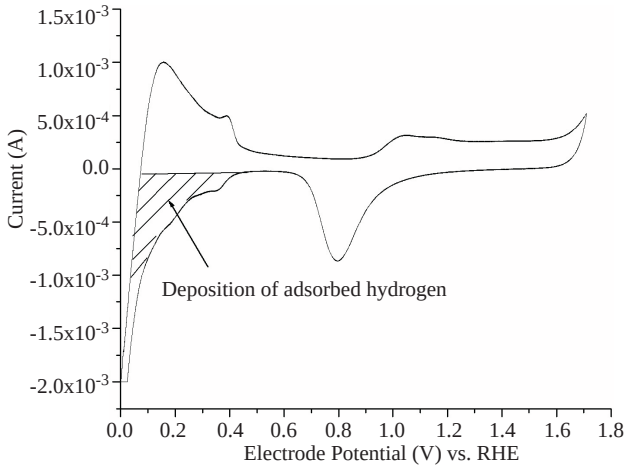

Figure 1. Cyclic voltammetry of polycrystalline platinum in 0.1 M H_2SO_4 at a scan rate of 100 mV/s.

A necessary quantitative evaluation of the chemically active surface area of the catalyst was determined from the H_{upd} charge. The H_{upd}charge was found from the cathodic potential sweep (0.4-0.05 V) during cyclic voltammetry in the acidic medium (Figure 1) by the charge transfer reaction (Volmer reaction) (Kinoshita *et al.*, 1986):

$$Pt + H^+ + e^- \leftrightarrow Pt - H_{ads} \tag{8}$$

After the integration of the area under the hydrogen deposition region (Figure 1) a total charge of 0.562 mC was obtained after subtracting the double layer contribution, the real Pt surface area Sreal = 0.562 mC/210 μC/cm^{-2}= 2.676 cm^2 and an H_{upd} monolayer adsorption charge of 210 μC/cm^{-2} on polycrystalline platinum were assumed. The integrated charge (corrected for double layer charging) can be related to the Pt surface area by assuming 210 μC/real cm^{2}Pt. The amount of surface Pt atoms ($N_{Pt,s}$) was calculated from Faraday's law for a one-electron reaction (Eq. (8)) $N_{Pt,s}$ = 0.562 mC/96,485 C/mol = 5.831 nmol. If the total number of platinum active sites is divided by the real surface (5.831 nmol/2.676 cm^2) it gives 2.9 nmol/cm^2, which corresponds finally to 1.2 atoms/Å^2(Wieckowski *et al.*, 2000).

Chronoamperometric experiments

In the chronoamperometry experiment, the potential was held constant and the resulting current transient was measured. When studying the electrooxidation of methanol, the chronoamperometry experiment begins with an electrode free of adsorbates that must be clean and activated (Melnick *et al.*, 2001). Therefore, in order to measure the current transients of methanol decomposition, the following program was implemented. First, 3 activating/cleaning potential steps between the onsets of hydrogen evolution (0.1 V vs. RHE) and the oxide region (1.4 V vs. RHE) were applied to the electrode. After a 100 ms pre-step from 0.1 to 1.4 V (3 times), the final step was to a measuring potential at which methanol decomposition was investigated (Wieckowski *et al.*, 2000). The oxidation currents were recorded for 1 s at the applied potential in a 0.5 M H_2SO_4 electrolyte for baseline correction and 0.5 M CH_3OH + 0.5M H_2SO_4 solution for methanol oxidation study. Each chronoamperometric experiment was repeated at least 10 times and corrected for the baseline and average current values. Standard deviations were within 10% for 10 chronoamperometric measurements (Tapan *et al.*, 2003). In this study all potentials were with respect to the reversible hydrogen electrode.

Results and Discussion

Reaction model

In order to simulate the methanol oxidation we made some assumptions in our reaction model. We assumed the adsorption of methanol is Langmuirian and all the intermediate species occupy a single site (each species can occupy only one site). Surface coverage cannot exceed one. Methanol oxidation was studied in the pure kinetic region by correcting the diffusion current (the pure kinetic region was regarded as the current regime where the current is 3 orders of magnitude lower than the diffusion controlled current (Hoster *et al.*, 2001); for 0.5 M CH_3OH solution diffusion effects are not negligible in the current range of 100 mA/cm^2).

We estimated the effect of diffusion on the total current and the diffusion coefficient for methanol in 0.5 M H_2SO_4 electrolyte solution on the platinum disk electrode. The steady state diffusion current (Bard and Faulkner, 2001) can be calculated from the following equation:

$$I_{ss} = 4.n.F.D_o.C_o.r_o \tag{9}$$

where r_o is the radius of the platinum disk, C_o is the initial methanol concentration and, D_o is the diffusion coefficient of methanol.

Derivation of model equations

In order to derive species balances we started with the definition of Faraday's law, where the current can be expressed in terms of the rate of change of electroactive species:

$$i = F.n_{eq}.\frac{dN}{dt} \tag{10}$$

where N is the number of moles of species, n_{eq} is the number of equivalence and F is Faraday's constant.

After that we converted the faradaic current in terms of the coverages of each electroactive species on the metal surface.

$$\frac{i}{F.n_{eq}.N_t} = \frac{d(N/N_t)}{dt} = \frac{d\theta_i}{dt} = \frac{A}{N_t}.(\sum \nu_i.k_i.\theta_i) \tag{11}$$

In Eq. (11), N_t represents the number of active metal surface atoms, θ_i represents the coverage of electroactive species, A is the area of the electrode, ν_i is the stoichiometric coefficient of input and output terms to the accumulation of species coverages, and k_i is the rate constant of the specific oxidation or adsorption reaction.

$$K_i = \frac{A.k_i}{N_t} \tag{12}$$

We can also define a rate constant term in terms of electrode area and the number of active metal sites, as in Eq. (12).

$$\frac{dC_{CH_3OH}}{dt} = -\theta_{pt} \cdot K_1 \cdot C_{CH_3OH} + K_{-1} \cdot \theta_{CH_3OH} \tag{13}$$

Equation (13) represents the accumulation term for methanol. The concentration term for methanol (C_{CH3OH}) was in fact defined as a coverage term for the dimensional consistency K_1 and K_{-1}terms (from Eq. (13)), the adsorption desorption rate constants.

$$\frac{d\theta_{CH_3OH}}{dt} = K_1.C_{CH_3OH}.\theta_{pt} - K_2.\theta_{CH_3OH}.\exp\left[\frac{(1-\beta)\cdot F\cdot\eta}{R\cdot T}\right] - K_{-1}.\theta_{CH_3OH} \tag{14}$$

Accumulation of surface methanol depends on the adsorption, desorption and electrochemical oxidation term, which was defined by the Butler-Volmer expression as given in Eq. (14). In Eq. (14), β represents a symmetric factor in the Butler-Volmer expression, which is approximated by 0.5 (Bard and Faulkner, 2001) for most electrochemical systems in the absence of actual measurements; η represents the overpotential during methanol oxidation, which is the difference between the applied potential and standard potential of the electrochemical reaction step (Table 1) (Tapan, 2003).

$$\frac{d\theta_{CH_3O}}{dt} = lK_2.\theta_{CH_3OH}.\exp\left[\frac{(1-\beta)\cdot F\cdot\eta}{R\cdot T}\right] - K_3.\theta_{CH_3O}.\exp\left[\frac{(1-\beta)\cdot F\cdot\eta}{R\cdot T}\right] \tag{15}$$

Equation (15) is a derivation for accumulation of surface methoxy species. Species balances (Eqs. (16), (17), (18), (19)) were derived for the other surface species.

Table 1. Standard potentials of reaction steps.

Reaction step	E° (V) vs. RHE
$CH_3OH \rightarrow CH_3O$	0.005
$CH_3O \rightarrow CH_2O$	0.005
$CH_2O \rightarrow CHO$	0.2257
$CHO \rightarrow CO$	0.2257
$CO \rightarrow CO_2$	0.346
H_2O (ads) $\leftrightarrow$ OH (ads) + H^+ + e	0.57

$$\frac{d\theta_{CH_2O}}{dt} = K_3.\theta_{CH_3O}.\exp\left[\frac{(1-\beta)\cdot F\cdot\eta}{R\cdot T}\right] - K_4.\theta_{CH_2O}.\exp\left[\frac{(1-\beta)\cdot F\cdot\eta}{R\cdot T}\right] \quad (16)$$

$$\frac{d\theta_{CHO}}{dt} = K_4.\theta_{CH_2O}.\exp\left[\frac{(1-\beta)\cdot F\cdot\eta}{R\cdot T}\right] - K_5.\theta_{CHO}.\exp\left[\frac{(1-\beta)\cdot F\cdot\eta}{R\cdot T}\right] \quad (17)$$

$$\frac{d\theta_{CO}}{dt} = K_5.\theta_{CHO}.\exp\left[\frac{(1-\beta)\cdot F\cdot\eta}{R\cdot T}\right] - K_7.\theta_{CO}.\theta_{H_2O}.\exp\left[\frac{(1-\beta)\cdot F\cdot\eta}{R\cdot T}\right] \quad (18)$$

$$\frac{d\theta_{H_2O}}{dt} = K_6.\theta_{pt}.C_{H_2O} - K_{-6}.\theta_{H_2O} - K_7.\theta_{CO}.\theta_{H_2O}.\exp\left[\frac{(1-\beta)\cdot F\cdot\eta}{R\cdot T}\right] \quad (19)$$

In Eq. (19), K_6 and K_{-6} represent the adsorption and desorption rate constants for the chemical activation of water on the platinum surface.

Since we assumed a monolayer coverage on the metal surface, the coverage of all surface species with vacant platinum sites should add up to one, as shown in Eq. (20) below

$$\theta_{Pt} + \theta_{CH_3OH} + \theta_{CH_3O} + \theta_{CH_2O} + \theta_{CHO} + \theta_{CO} = 1 \quad (20)$$

If we take the derivative of Eq. (20), the change in vacant platinum sites with respect to time becomes:

$$\frac{d\theta_{pt}}{dt} = -\frac{d\theta_{H_2O}}{dt} - \frac{d\theta_{CO}}{dt} - \frac{d\theta_{CHO}}{dt} - \frac{d\theta_{CH_2O}}{dt} - \frac{d\theta_{CH_3O}}{dt} - \frac{d\theta_{CH_3OH}}{dt} \quad (21)$$

if we evaluate the faradaic currents of each electrochemical reaction step according to the reaction scheme (Eqs. (22)-(26)) below

$$CH_3OH.Pt \xrightarrow{K_2} CH_3O.Pt + e^- \quad (22)$$

$$CH_3O.Pt \xrightarrow{K_3} CH_2O.Pt + e^- \quad (23)$$

$$CH_2O.Pt \xrightarrow{K_4} CHO.Pt. + e^- \quad (24)$$

$$CHO.Pt \xrightarrow{K_5} CO.Pt + e^- \quad (25)$$

$$CO.Pt + H_2O.Pt \xrightarrow{K_7} CO_2 + 2.Pt + 2H^+ + 2e^- \quad (26)$$

The equations (Eqs. (27)-(31)) become
First decomposition of methanol

$$I_1 = n_{eq}.Nt.F.K_2.\theta_{CH_3OH}.\exp\left[\frac{(1-\beta)\cdot F\cdot\eta}{R\cdot T}\right] \quad (27)$$

Second decomposition of methanol

$$I_2 = n_{eq}.Nt.F.K_3.\theta_{CH_3O}.\exp\left[\frac{(1-\beta)\cdot F\cdot\eta}{R\cdot T}\right] \quad (28)$$

Third decomposition of methanol

$$I_3 = n_{eq}.Nt.F.K_4.\theta_{CH_2O}.\exp\left[\frac{(1-\beta)\cdot F\cdot\eta}{R\cdot T}\right] \quad (29)$$

Surface CO formation

$$I_4 = n_{eq}.Nt.F.K_5.\theta_{CHO}.\exp\left[\frac{(1-\beta)\cdot F\cdot\eta}{R\cdot T}\right] \quad (30)$$

Water-gas shift reaction

$$I_5 = n_{eq}.Nt.F.K_7.\theta_{CO}.\theta_{H2O}.\exp\left[\frac{2.(1-\beta)\cdot F\cdot\eta}{R\cdot T}\right] \quad (31)$$

Finally, all these faradaic current steps can be summed up to derive the total faradaic current due to the decomposition process of methanol and the water-gas-shift reaction.

Total faradaic current becomes

$$I_T = I_1 + I_2 + I_3 + I_4 + I_5 \tag{32}$$

The total faradaic current given by Eq. (32) was a result of numerical integration from the simulation. Rate constants were determined by pseudo steady state hypothesis and expected time dependence of surface species was obtained by the simulation of the proposed mechanism.

Derivation of pseudo steady state equations

In order to determine electrokinetic rate constants for an assumed methanol electro-oxidation mechanism, we applied the pseudo steady state hypothesis (Fogler, 1999). For the pseudo steady state model, we assumed that the accumulation of all surface species is zero:

$$\sum_{i=1}^{n} \frac{d\theta_i}{dt} = 0 \tag{33}$$

Since the methanol concentration is in excess, oxidation would not change the concentrations in short chronoamperometric experiments. Using Eq. (33) we derived the steady state coverages of surface species in terms of initial concentrations of methanol in the electrolyte solution as shown below

$$\theta_{CH_3OH} = \frac{k_1 * \theta_{pt} * C_{CH3OH}}{k_{-1} + k_2 * \exp\left[\frac{(1-\beta)*F*\eta_1}{R*T}\right]} = B * \theta_{pt} \tag{34}$$

$$\theta_{CH3O} = \frac{k_2 * k_1 * \theta_{pt} * C_{CH3OH}}{k_3 * \left[k_{-1} + k_2 * \exp\left[\frac{(1-\beta)*F*\eta_1}{R*T}\right]\right]} * \exp\left[\frac{(1-\beta)*F*(\eta_1-\eta_2)}{R*T}\right] = C * \theta_{pt} \tag{35}$$

$$\theta_{CHO} = \frac{k_2}{k_5} * \frac{k_1 * \theta_{pt} * C_{CH3OH}}{\left[k_{-1} + k_2 * \exp\left[\frac{(1-\beta)*F*\eta_1}{R*T}\right]\right]} * \exp\left[\frac{(1-\beta)*F*(\eta_1-\eta_2)*(\eta_2-\eta_3)*(\eta_3-\eta_4)}{R*T}\right] = E * \theta_{pt} \tag{36}$$

$$\theta_{CO} = \frac{k_2 * k_1 * C_{CH3OH} * \exp\left[\frac{(1-\beta)*F*(\eta_1-\eta_2)*(\eta_2-\eta_3)*(\eta_3-\eta_4)*(\eta_4-\eta_5)}{R*T}\right] * \left[k_{-6} + k_7 * \theta_{CO} * \exp\left[\frac{(1-\beta)*F*\eta_5}{R*T}\right]\right]}{k_7 * k_6 * C_{H2O} * \left[k_{-1} + k_2 * \exp\left[\frac{(1-\beta)*F*\eta_1}{R*T}\right]\right]} \tag{37}$$

$$\theta_{CO} = \theta_{pt} * A \tag{38}$$

$$\theta_{H2O} = \frac{\theta_{pt} * k_6 * C_{H2O}}{\left[k_{-6} + k_7 * \left[\frac{A*k_{-6}}{1-A*k_7*\exp\left[\frac{(1-\beta)*F*\eta_5}{R*T}\right]}\right]\right] * \exp\left[\frac{(1-\beta)*F*\eta_5}{R*T}\right]} \tag{39}$$

$$\theta_{H2O} = G * \theta_{pt} \tag{40}$$

In these equations the concentrations of methanol and water were assumed to be constant because these species are in excess in the electrolyte and the oxidation would not affect their concentration in short chronoamperometric experiments. Since we assumed that there is a monolayer coverage of all species and all the surface coverages should add up to 1:

$$\theta_{pt} + \theta_{CH3OH} + \theta_{CH3O} + \theta_{CH2O} + \theta_{CHO} + \theta_{CO} + \theta_{H2O} = 1 \tag{41}$$

substituting the intermediate coverages in Eq. (41), we obtain the expression for the vacant platinum sites:

$$\theta_{pt} = \frac{1 - \frac{A*k_{-6}}{\left[1 - A*k_7*\exp\left[\frac{(1-\beta)*F*\eta_5}{R*T}\right]\right]}}{(1 + B + C + D + E + G)} \tag{42}$$

The expressions for the steady state currents for various reaction steps are given as

$$I_1st = Nt * F * neq * k_2 * \theta_{CH3OHst} * \exp\left[\frac{(1-\beta) * F * \eta_1}{R * T}\right] \tag{43}$$

$$I_2st = Nt * F * neq * k_3 * \theta_{CH3O} * \exp\left[\frac{(1-\beta) * F * \eta_2}{R * T}\right] \tag{44}$$

$$I_3st = Nt * F * neq * k_4 * \theta_{CH2O} * \exp\left[\frac{(1-\beta) * F * \eta_3}{R * T}\right] \tag{45}$$

$$I_4st = Nt * F * neq * k_5 * \theta_{CHO} * \exp\left[\frac{(1-\beta) * F * \eta_4}{R * T}\right] \tag{46}$$

$$I_5st = Nt * F * neq * k_7 * \theta_{CO} * \theta_{H2O} * \exp\left[\frac{2 * (1-\beta) * F * \eta_5}{R * T}\right] \tag{47}$$

When all the steady state currents were added up to form the total steady state current, a non-linear algebraic equation was obtained. Non-linear regression analysis was applied to find the electrochemical rate constants (K_1 through K_7) by fitting the total currents (derived from PSSH) with the steady state currents (from chronoamperometry) at different applied potentials (<0.6 V). Total steady state current is defined similar to Eq. (32).

$$I_{st}total = I_1st + I_2st + I_3st + I_4st + I_5st + Id \tag{48}$$

where I_d shows the diffusion current in Eq. (48).

The initial estimates and the order of magnitude of rate constants (K_1 through K_7) should be selected properly by trial and error so that the percent error and the residuals can be minimized.

The results of non-linear regression analysis are given in Table 2. There is decent agreement between the experimental and theoretical results. The model predicts the experimental behavior best before 0.452 V and after 0.472 V; between 0.452 V and 0.472 V; the current-voltage behavior suddenly changes but follows normal behavior after 0.472 V (Figure 2).

Table 2. Comparison of experimental and model steady state currents.

Cell potential (V)	I^*_{ss} (experimental)(A)	I_{ss} (model)(A)	% error
0.348	3.11×10^{-5}	3.166×10^{-5}	1.814
0.392	4.08×10^{-5}	4.08×10^{-5}	3.556×10^{-3}
0.442	4.22×10^{-5}	4.674×10^{-5}	10.766
0.452	5.979×10^{-5}	4.752×10^{-5}	20.521
0.462	5.851×10^{-5}	4.821×10^{-5}	17.605
0.472	5.683×10^{-5}	4.883×10^{-5}	14.079
0.492	5.227×10^{-5}	4.994×10^{-5}	4.47
0.542	5.1×10^{-5}	5.278×10^{-5}	3.485
0.592	5.468×10^{-5}	5.804×10^{-5}	6.136

* Steady state current

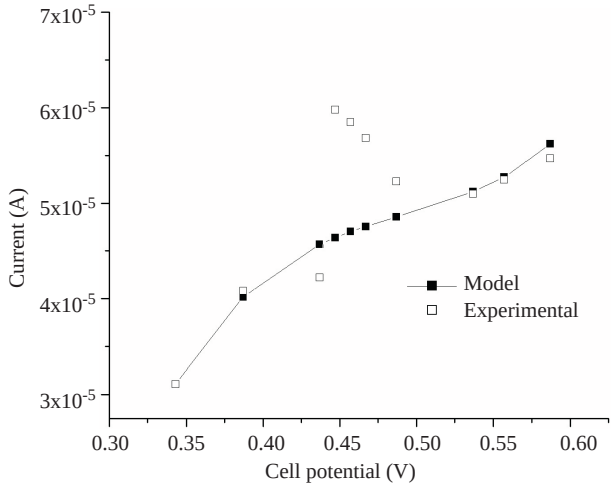

Figure 2. Comparison of experimental and model steady state currents at different applied potentials.

The diffusion coefficient of methanol calculated based on our data was 3.11×10^{-11} cm^2/s, and the steady state diffusion current was 7.1×10^{-2} mA/cm^2, which made a contribution of maximum ∼2% to the total current. Current limitation by mass transport is unlikely for methanol concentrations of 0.5 M unless the current densities are in the range of 100 mA/cm^2 giving a diffusion coefficient of 10^{-5}cm^2/s as we have previously described. Our model showed that diffusion effects on the total current were negligible (Hoster *et al.*, 2001).

Non-linear regression resulted in the rate constants shown in Table 3. After the error analysis, we also determined the steady state values for the surface species and steady state currents for the decomposition and CO oxidation steps. Figure 3 shows that as the cell potential increased, the water adsorption on the platinum increases from ∼0.8 to 0.999 and CO coverages decrease from ∼0.2 to 0.001. It was also reported on Pt/C catalyst layers that increasing potentials from 0.3 to 0.4 V vs. RHE decreased steady state CO coverage linearly (Madden and Stuve, 2003). Water coverage became almost constant and independent of applied potential before E < 0.6 V vs. RHE. Water adsorption on platinum before E < 0.6 V vs. RHE was also reported as an independent mechanism of applied potential, forming one-dimensional water chains (Futnikov *et al.*, 1995). Free platinum sites also increased with the cell potential. Just after potentials E = 0.35 V vs. RHE it was seen that water almost covered all the platinum surface and only a small percentage of the active surface was available for other surface species. 0.35 V vs. RHE was also regarded as a critical potential after which the first CO_2 formation was observed (Leger, 2001). In Figure 4, first and second decomposition currents have the highest values at all potentials, and they are most probably dominant (fastest steps) before E < 0.6 V. According to the model before 0.45 V the water-gas shift reaction gives the lowest currents, and after 0.45 V the rate-limiting step changes to third decomposition and carbon monoxide formation steps. As the cell potential was increased, the water-gas shift reaction leading to carbon monoxide removal also increased.

Dynamic profiles

Rate constants determined from PSSH after nonlinear regression were applied to our dynamic model, and then the current and coverage profiles were observed in the potential range 0.348-0.592 V. Almost 90% of the platinum surface was covered with water at all of the applied potentials. The order and magnitude of decomposition products change with the applied potential as well. CO, CHO, CH_2O coverage increased while methanol and methoxy coverage de-

creased with the applied potential (Figure 5). When the current profiles were determined, it was seen that the decomposition rates reached the same value and the water-gas shift reaction rate increased with the applied potential (Figure 6).

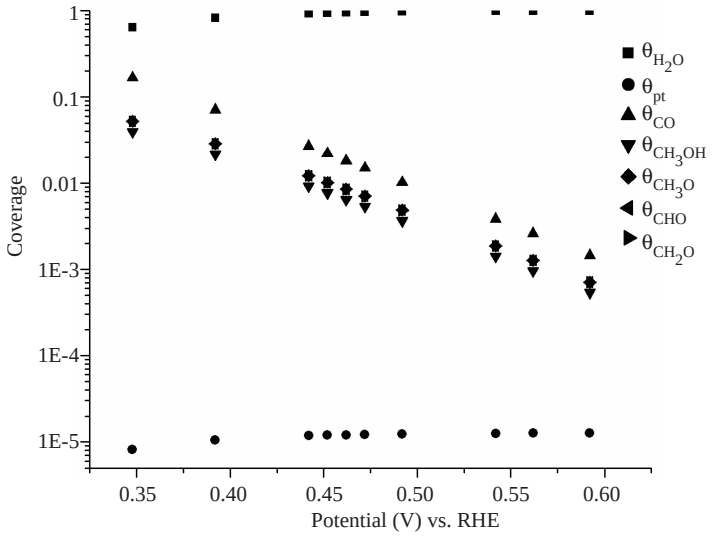

Figure 3. Steady state coverage profiles at an applied cell potential.

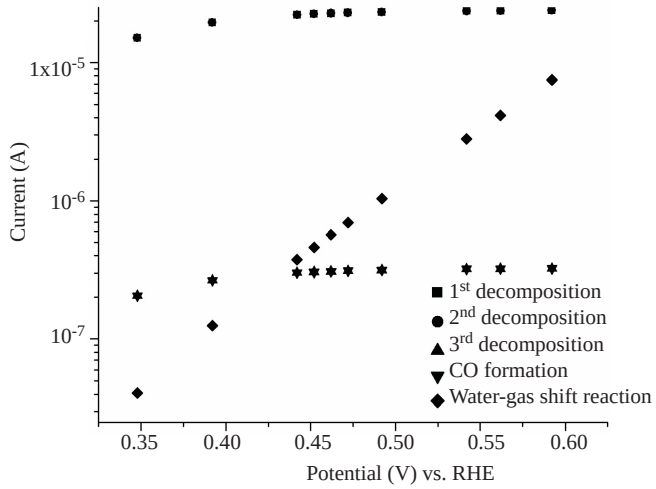

Figure 4. Steady state current profiles at an applied cell potential.

Table 3. Estimation of rate constants by non-linear regression.

Rate constant	Value
$K_1(\text{coverage}^{-1}.s^{-1})$	9.808×10^{-4}
$K_{-1}(s^{-1})$	0.044
$K_2(s^{-1})$	6.053×10^{-4}
$K_3(s^{-1})$	6.433×10^{-4}
$K_4(s^{-1})$	6.439×10^{-4}
$K_5(s^{-1})$	6.433×10^{-4}
$K_6(\text{coverage}^{-1}.s^{-1})$	2.795×10^{-5}
$K_{-6}(s^{-1})$	0.133
$K_7(\text{coverage}^{-1}.s^{-1})$	5.268×10^{-4}

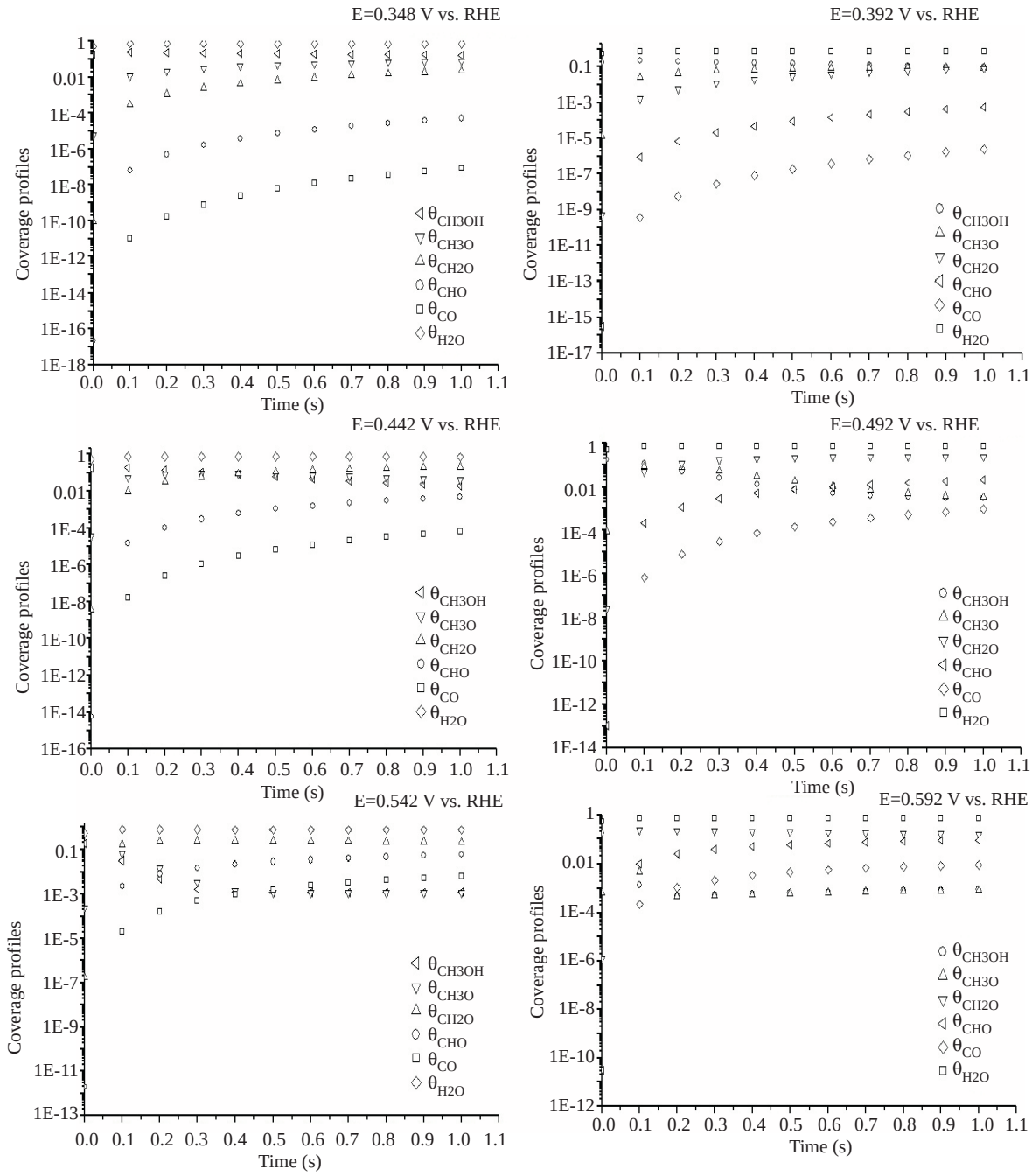

Figure 5. Dynamic coverage profiles at different applied potentials E=0.348-0.592 V vs. RHE.

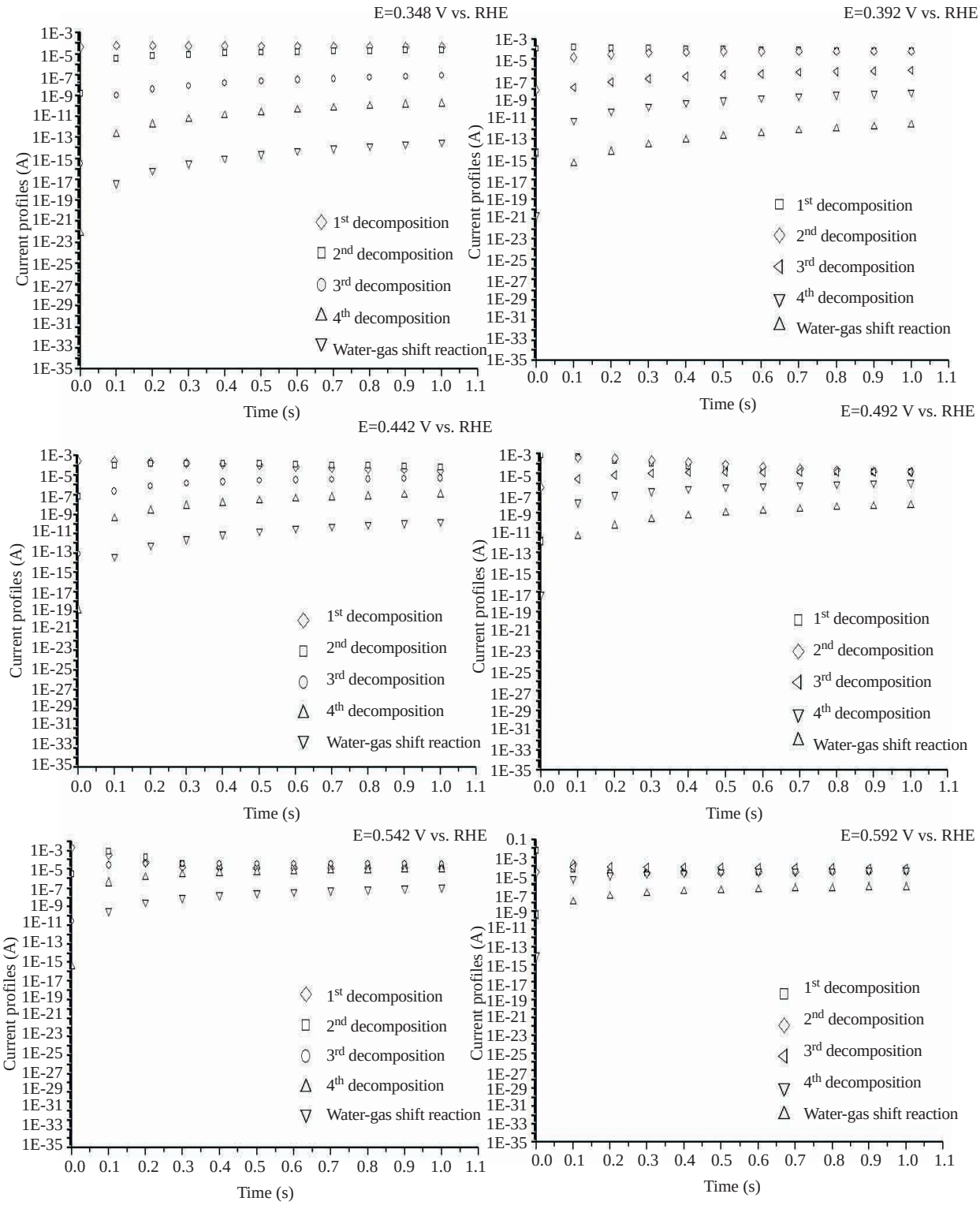

Figure 6. Dynamic current profiles at different applied potentials E = 0.348-0.592 V vs. RHE.

The CO profile showed that the poisoning trend changed at potentials close to 0.6 V vs. RHE, but the dynamic profile showed that the water-gas shift reaction has no effect during 1 s of oxidation (Figure 7).

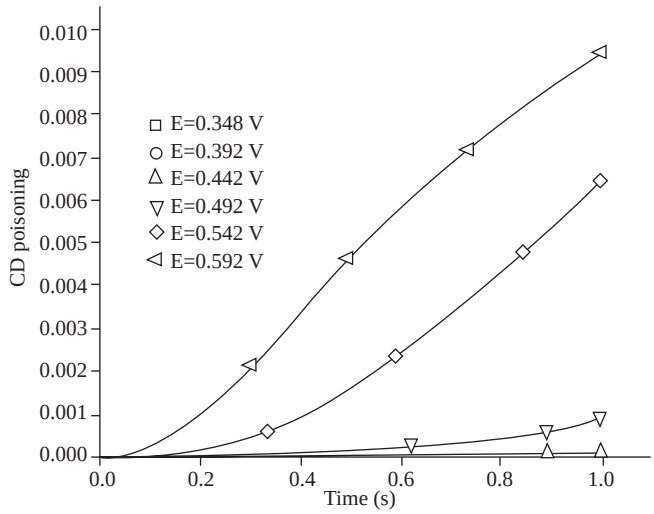

Figure 7. CO profiles at different potentials before < 0.6V vs. RHE.

When the PSSH model was compared with the dynamic model (after 1 s), we observed that in the latter coverage profiles differ, and CO, CHO and CH_2O show increasing functions, unlike the former. For oxidation times exceeding 1 s the effect of the water-gas shift reaction can be seen more clearly with a drop in CO poisoning. For the water-gas shift reaction to be effective, dynamic model shows that methanol oxidation should exceed 1 s (Figure 8).

Two critical potentials, 0.542 V and 0.45 V, were observed in this work. Before 0.542 V, the methanol decomposition activity exceeded the water-gas shift reaction, which led to low coverage of carbon monoxide and high coverage of surface decompositon products. An increase in potential changed the surface activity in favor of the water-gas shift reaction, while decomposition rates started to reach a constant value. At 0.542 V all rates became equal except for the water-gas shift reaction, which was still increasing. This leads to coverage distribution on the surface changing dramatically (see Table 4). When the steady state values were considered, after 0.45 V, the water-gas shift reaction changed its order, exceeding the third decomposition and CO formation rates (see Figure 4). However, this did not change the surface coverage distribution until 0.6 V (see Figure 3 and Table 5). Steady state profiles showed that the water-gas shift reaction was always effective (showing a CO coverage drop) until 0.6 V, with a critical potential of 0.45 V (Figure 3). On the other hand, dynamic profiles showed that the water-gas shift reaction was not effective on CO removal before 1 s (Figure 5), although its rate increased with the applied potential. The critical potential (0.542 V vs. RHE) showed that CO coverage exceeded methanol and methoxy coverage when decomposition reaction rates reached a constant value (Figure 6).

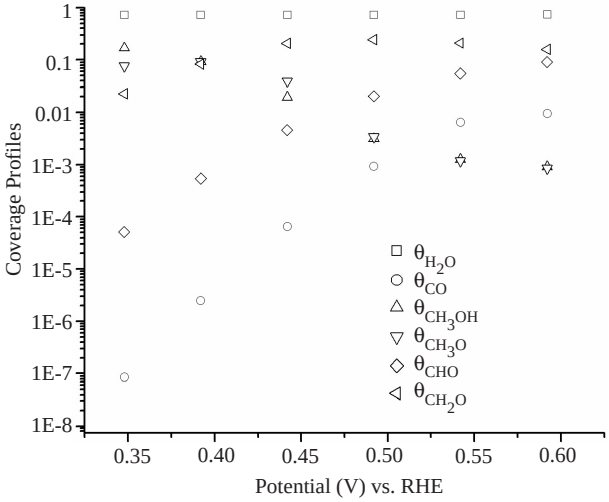

Figure 8. Coverage profiles after 1 s from the dynamic model.

Table 4. Order of magnitude of coverages with respect to applied potential (before 1 s).

Applied potential (V) vs. RHE	Order of Coverages
0.348	$\theta_{CO} < \theta_{CHO} < \theta_{CH2O} < \theta_{CH3O} < \theta_{CH3OH} < \theta_{H2O}$
0.392	$\theta_{CO} < \theta_{CHO} = \theta_{CH2O} = \theta_{CH3O} = \theta_{CH3OH} < \theta_{H2O}$
0.442	$\theta_{CO} < \theta_{CHO} < \theta_{CH3OH} < \theta_{CH3O} < \theta_{CH2O} < \theta_{H2O}$
0.492	$\theta_{CO} < \theta_{CHO} = \theta_{CH3O} < \theta_{CHO} < \theta_{CH2O} < \theta_{H2O}$
0.542	$\theta_{CH3O} = \theta_{CH3OH} < \theta_{CO} < \theta_{CHO} < \theta_{CH2O} < \theta_{H2O}$
0.592	$\theta_{CH3O} = \theta_{CH3OH} < \theta_{CO} < \theta_{CHO} = \theta_{CH2O} < \theta_{H2O}$

Table 5. Order of magnitude of coverages with respect to applied potential (at steady state).

Applied potential (V) vs. RHE	Order of Coverages
0.348	$\theta_{CHO} = \theta_{CH2O} = \theta_{CH3O} = \theta_{CH3OH} = \theta_{CO} < \theta_{H2O}$
0.392	$\theta_{CHO} = \theta_{CH2O} = \theta_{CH3O} = \theta_{CH3OH} = \theta_{CO} < \theta_{H2O}$
0.442	$\theta_{CHO} = \theta_{CH2O} = \theta_{CH3O} = \theta_{CH3OH} = \theta_{CO} < \theta_{H2O}$
0.492	$\theta_{CHO} = \theta_{CH2O} = \theta_{CH3O} = \theta_{CH3OH} = \theta_{CO} < \theta_{H2O}$
0.542	$\theta_{CHO} = \theta_{CH2O} = \theta_{CH3O} = \theta_{CH3OH} = \theta_{CO} < \theta_{H2O}$
0.592	$\theta_{CHO} = \theta_{CH2O} = \theta_{CH3O} = \theta_{CH3OH} = \theta_{CO} < \theta_{H2O}$

Conclusions

Our pseudo steady state model predicted reasonable values for the steady state currents. The model also predicted that at E < 0.6 V the water gas shift reaction can explain the methanol oxidation. The model showed that increasing the anodic potential increases the water adsorption and reduces the surface poisoning. First and second decomposition of methanol were the fastest (dominant) steps before 0.6 V with the highest steady state currents and after 0.45 V the rate determining step shifted from a water-gas shift reaction to third decomposition and CO formation. The dynamic profile of surface poisoning provided a good insight to water-gas shift reaction. The result of the 1-s simulation showed that surface CO, CHO and CH_2O show completely different profiles from PSSH. The water-gas shift reaction was always the rate determining step in the potential range studied with oxidation times 1 s.

Nomenclature

β	symmetric factor
η_1	overpotential for the first decomposition of methanol
η_2	overpotential for the second decomposition of methanol
η_3	overpotential for the third decomposition of methanol
η_4	overpotential for the formation of carbon monoxide
η_5	overpotential for the oxidation of carbon monoxide
η	overpotential V
θ_i	coverage
C_i	concentration of species (sites/cm^3)
Do	methanol diffusion coefficient (cm^2/s)
E	applied potential (V)
E_{eq}	equilibrium potential (V)
F	Faraday's constant 96,500 coulomb/mole equivalent
I	current A
K	rate constant s^{-1}
K1	methanol adsorption rate constant (coverage^{-1}.s^{-1})
K11	methanol desorption rate constant (s^{-1})
K2	OH bond breakage rate constant (s^{-1})
K3	2^{nd} decomposition rate constant (s^{-1})
K4	3^{rd} decomposition rate constant (s^{-1})
K5	CO formation rate constant (s^{-1})
K6	water activation rate constant (coverage^{-1}.s^{-1})
K66	water de-activation rate constant (s^{-1})
K7	CO oxidation rate constant (coverage^{-1}.s^{-1})
n_{eq}	# of equivalence
R	ideal gas constant kJ/mol.K
RHE	reversible hydrogen electrode
ro	radius of platinum disk electrode (cm)

References

Bagotzky, V.S., Vasiliev, Yu. B. and Khazova, O.A., "Generalized Scheme of Chemisorption, Electrooxidation and Electroreduction of Simple Organic Compounds on Platinum Group Metals", Journal of Electroanalytical Chemistry, 81, 229-238, 1977.

Bard, A.J. and Faulkner, L.R., "Electrochemical Methods: Fundamentals and Applications", 2^{nd} edition, John Wiley & Sons Inc., New York, 172, 2001.

Beden, B., Lamy, C. and Leger J.M., Modern Aspects of Electrochemistry, (ed. Bockris, J.O' M., Conway, B.E. and White, R.E.) Plenum Press, New York, 22, 97-264, 2001.

Ehlers, D.H., Spitzer, A. and Luth, H., "The Adsorption of Methanol on Pt (111), on IR Reflection and U.V. Photoemission Study", Surface Science, 160, 57-69, 1985.

Fogler, H.S., "Elements of Chemical Reaction Engineering", 3^{rd} edition, Prentice Hall International Series in the Physical and Chemical Engineering Series, New Jersey, 342, 616, 1999.

Franaszczuk, K., Herrero, E., Zelenay, P., Wieckowski, A., Wang, J. and Masel, R.I., "A Comparison of Electrochemical and Gas Phase Decomposition of Methanol on Platinum Surfaces", Journal of Physical Chemistry, 96, 8509, 1992.

Futnikov, A.M., Linke, U., Stimming, U. and Vogel., "An In-situ STM Study of Anion Adsorption on Pt(111) from Sulfuric Acid Solutions" Surface Science, 324, L343-L348, 1995.

Hoster, H., Iwasita, T., Baumgartner, H. and Vielstich, W., "Current-Time Behavior of Smooth and Porous PtRu Surfaces for Methanol Oxidation", Journal of the Electrochemical Society, 148, A496-A501, 2001.

Jarvi, T.D., Sriramulu, S. and Stuve, E.M., "Potential Dependence of the Yield of Carbon Dioxide from Electrocatalytic Oxidation of Methanol on Platinum (100)", The Journal of Physical Chemistry B, 101, 3649-3652, 1997.

Kinoshita, K. and Stonehart, P., (ed: Bockris, J.O'M. and Conway, B.E.), Modern Aspects of Electrochemisty (no. 12), Plenum, New York 1986, p. 228.

Leger, J.M., "Mechanistic Aspects of Methanol Oxidation on Platinum-Based Electrocatalysts", Journal of Applied Electrochemistry, 31, 767-771, 2001.

Lamy, C., Leger J-M. and Srinivasan S., Modern Aspects of Electrochemistry, (ed. Bockris, J.O'M., Conway, B.E. and White, R.E.) Plenum Press, New York, 34, 53-118, 2001.

Lipkowski, J. and Ross, P.N., Electrocatalysis, Wiley-VCH, New York, 90-103, 2001.

Madden, H.T. and Stuve, E.M., "Mechanisms of Elevated Temperature Methanol Electro-oxidation and Poisoning on Pt'C-Nafion Catalyst Layers", Journal of the Electrochemical Society, 150, E571-E577, 2003.

Melnick R. and Palmore T., "Time-Dependent Impedance of the Electro-oxidation of Methanol on Polished Polycrystalline Platinum", Journal of Physical Chemistry B, 105, 9449-9457, 2001.

Prakash, J. and Joachin, H., "Electrocatalytic Activity of Ruthenium for Oxygen Reduction in Alkaline Solution", Electrochimica Acta, 45, 2289-2296, 2000.

Tapan, N.A., "Investigation of Methanol Oxidation Electrokinetics on Catalytic Surfaces" Illinois Institute of Technology, Ph.D. Thesis, 2003.

Vieltich, W. and Xia, X.H., "Comments on Electrochemistry of Methanol at Low Index Crystal Planes of Platinum: An Integrated Voltammetric and Chronoamperometric Study", Journal of Physical Chemistry, 99, 10421-10422, 1995.

Wieckowski, A., Chrzanowski W. and Lu, G.Q., "Catalytic Methanol Decomposition Pathways on a Platinum Electrode", Journal of Physical Chemistry B, 104, 5566-5572, 2000.